Mathematical Modelling and Numerical Simulation with Applications, 2022, 2(4), 228–243

https://www.mmnsa.org
ISSN Online: 2791-8564 / Open Access
https://doi.org/10.53391/mmnsa.2022.019

RESEARCH PAPER

Dynamics of a fractional-order COVID-19 model under the nonsingular kernel of Caputo-Fabrizio operator

Saeed Ahmad [1,†], Dong Qiu [2,3,†] and Mati ur Rahman [4,†,*]

[1]Department of Mathematics, University of Malakand, Chakdara Dir (L), KP, Pakistan, [2]School of Mathematics and Information Science, Guangxi University, No. 100, East University Road, Nanning, 530004, P.R. China, [3]College of Science, Chongqing University of Posts and Telecommunications, Nanan, 400065, Chongqing, China, [4]School of Mathematical Science, Shanghai Jiao Tong University, P.R. China

*Corresponding Author
†saeedahmad@uom.edu.pk (Saeed Ahmad); qiudong@cqupt.edu.cn (Dong Qiu); mati-maths_374@sjtu.edu.cn (Mati ur Rahman)

Abstract

For the sake of human health, it is crucial to investigate infectious diseases including HIV/AIDS, hepatitis, and others. Worldwide, the recently discovered new coronavirus (COVID-19) poses a serious threat. The experimental vaccination and different COVID-19 strains found around the world make the virus' spread unavoidable. In the current research, fractional order is used to study the dynamics of a nonlinear modified COVID-19 SEIR model in the framework of the Caputo-Fabrizio fractional operator with order b. Fixed point theory has been used to investigate the qualitative analysis of the solution respectively. The well-known Laplace transform method is used to determine the approximate solution of the proposed model. Using the COVID-19 data that is currently available, numerical simulations are run to validate the necessary scheme and examine the dynamic behavior of the various compartments of the model. In order to stop the pandemic from spreading, our findings highlight the significance of taking preventative steps and changing one's lifestyle.

Key words: COVID-19 model; theoretical analysis; Laplace transform; Caputo-Fabrizio fractional operator; numerical simulations
AMS 2020 Classification: 37N25; 34A25; 44A10

1 Introduction

Since December 2019, the whole globe has been facing the dangerous and contagious new infection COVID-19. The infection has caused a lot of health, mental, economic, and unemployment problems throughout the globe. According to recent reports, over fifty million individuals are infected, and nearly four and a half million people have died from the said infection [1]. Pakistan has also been severely affected by COVID-19, with approximately 23,000 citizens dying and 1.5 million contracting the infection. Due to these circumstances, each and every country develops its own policy for controlling the pandemic. For this reason, they ban overcrowding in air transportation services, bus services, and various educational institutions. Different immigration services among the countries are also banned by the policymakers of each country. The big cause of this infection is the meeting of

➤ **Received:** 17.11.2022 ➤ **Revised:** 25.12.2022 ➤ **Accepted:** 27.12.2022 ➤ **Published:** 29.12.2022

infectious people with an uninfected population. Therefore keeping masks is also the cry of the day for reducing the transmission of COVID-19. Beyond this, some other precautionary measures are also taken by different countries [2].

The said pandemic is a cause of fear for humanity throughout the world, as most people are aware of past pandemics from which a considerable number of the population faced death. Technology advances over time, allowing for the cure and treatment of various epidemics. To overcome an epidemic, vaccines are prepared in the laboratory. Each related field of science plays a role in the establishment of control strategies, and among them is mathematical modeling. Mathematical modeling gives a prediction of various diseases by using past and future data. For the first time, a real-world problem had been studied via mathematical expressions in the eighteenth century. Following that, mathematical modelling has made significant contributions to the investigation of a wide range of real-world problems [3, 4, 5, 6].

Recently, the pandemic of COVID-19 has attracted the focus of many researchers in various fields as can be seen in [7, 8, 9, 10]. Mathematicians also played a role in the investigation of the said pandemic. The said disease has been transformed into mathematical expressions, and future predictions have been reported. Useful information about the past and present of the disease has been reported, which is advantageous in establishing control strategies for its eradication from society. In this regard, valuable work can be found in [11, 12, 13, 14, 15, 16]. The formation of a mathematical formula consists of conditions regarding the parameters involved in the problem under consideration. Various mathematical models exist in the literature that are helpful in understanding the spread of COVID-19 and suggest the adoption of policies necessary to control (optimize) the spread of the infection in an effective way. One of such remarkable models has been reported by [17]. The authors classified the total population into six categories. These includes the susceptible class $\tilde{\mathbb{S}}$, the latently infected compartment $\tilde{\mathbb{E}}$, the infected class $\tilde{\mathbb{I}}$, the class of recovered population $\tilde{\mathbb{R}}$, the demised class $\tilde{\mathbb{D}}$ and $\tilde{\mathbb{M}}$ is the COVID-19 filthy materials or surfaces in the atmosphere. The model reported in [17] has been expressed in the form of the following system of autonomous differential equations:

$$\begin{aligned}
\frac{d\tilde{\mathbb{S}}}{dt} &= \Pi - (\tau + \alpha_1 + \beta q)\tilde{\mathbb{S}},\\
\frac{d\tilde{\mathbb{E}}}{dt} &= \beta q\tilde{\mathbb{S}} - (\vartheta + (1-\kappa)\tau + \alpha_1)\tilde{\mathbb{E}},\\
\frac{d\tilde{\mathbb{I}}}{dt} &= \tau\tilde{\mathbb{S}} + (1-\kappa)\tau\tilde{\mathbb{E}} - (\rho + \alpha_1 + \upsilon)\tilde{\mathbb{I}},\\
\frac{d\tilde{\mathbb{R}}}{dt} &= \vartheta\tilde{\mathbb{E}} + \upsilon\tilde{\mathbb{I}} - \alpha_1\tilde{\mathbb{R}},\\
\frac{d\tilde{\mathbb{D}}}{dt} &= \rho\tilde{\mathbb{I}} - \alpha_2\tilde{\mathbb{D}},\\
\frac{d\tilde{\mathbb{M}}}{dt} &= \sigma\tilde{\mathbb{E}} + \zeta\tilde{\mathbb{I}} - \varphi\tilde{\mathbb{M}},
\end{aligned} \tag{1}$$

In model (1), the parameter description has been given in Table 1.

Parameters	values
Π	The rate of recruitment of susceptible class
α_1	Natural death rate except for dead population
α_2	Burning the carcass of dead population
ρ	The demise rate due to virus
ϑ	The rate of recovery from the infection
κ	The rate of average effectiveness of prevailing self-precautionary measures
φ	The rate of decay of $\tilde{\mathbb{M}}$
ζ	The transfer rate from $\tilde{\mathbb{I}}$ to environment
τ	The rate of force of infection
β	The dissemination rate of susceptible class
q	The rate of change of behavior function
υ	The rate of recovered persons fro exposed class
σ	The shedding rate from $\tilde{\mathbb{E}}$ to environment

Table 1. Description of the given parameters

Fractional calculus (FC), which has a wide range of applications in the modelling of physical processes, has grown in popularity among scholars over the past few decades. The ideas of classical calculus are made more universal by FC. Riemann-Liouville and Caputo conducted the initial investigation into the generalization of the ordinary integral and differential operators into fractional derivatives (FD) [18, 19]. After that, the fractional operator has been used by several researchers in a variety of sectors of science, engineering, and real-world issues [20, 21, 22]. In order to explore real-world issues including viscoelasticity systems, signal processing, diffusion processes, and control processing, fractional order differential equations provided a suitable framework, interested readers are directed to [23, 24, 25, 26]. Recently, in 2015 Caputo and Fabrizio introduced a new concept of fractional order derivative which has a non-singular kernel [27]. Several researchers have published many articles on this new concept of fractional derivatives; for instance, see [28, 29, 30]. The subject has been handled from a variety of angles, including quantitative analysis that considers existence, uniqueness, and regularity, as well as a numerical, analytical method, and the Laplace transform method to evaluate and interpret the data [31, 32, 33].

FC operators have more widespread advantages than the integer order operator since their nonlocal kernels are defined. The memory and history of any physical process are preserved by the fractional operators (FOs). The convolution of the kernels is a

topic of interest to many FOs. Numerous research publications have demonstrated the advantages of FOs over traditional operators. We go over some uses of FOs for the mathematical modelling of actual physical issues. According to the authors in [34], research was done on the COVID-19 pandemic disease's fractional-order mathematical model, which was based on actual data. Authors in [35], based on actual clinical data, examined the human liver in fractional order. The authors in [36], examined three different fractional operators on the blood ethanol model. For modelling bacterial infections, specifically, researchers also employ FOs. The authors in [37] assessed the Salmonella bacterial infection using fractional operators. The authors in [38] using nonsingular fractional operators, the risky bacterial infection (Dengue fever) was studied. A significant amount of work has been done by researchers in the applications of FC and applied sciences [39, 40, 41, 42].

The motivation and novelty of our work are inspired by the above literature, we study a system of COVID-19 using Caputo-Fabrizio fractional derivative with the exponential kernel. We develop the theoretical results of the considered system. To observe the dissimilarity among the results of the fractional-order and classical models, we compare the concerning results. The obtained results reveal that the analysis obtained from the innovative fractional derivative is more conclusive compared with the analysis of classical derivatives.

The structure of this manuscript is as follows. In Section 2 we recall basic results and notations from FC. In Section 3, we develop the qualitative results for the system under investigation. In section 4, using the well-known Laplace transform together with the integral of Laplace, we find the numerical solution of the model under study. Taking into account the data available in the literature, we carry out numerical simulations in Section 5 and represent simulations graphically. At the end, we conclude our findings in Section 6.

2 Preliminaries

Here, we present some basic definitions from the literature.

Definition 1 *[27] Let a function be $g \in H^1[0,T]$, where $T > 0$, and $b \in (0,1)$, then the fractional Caputo-Fabrizio CF derivative is given by*

$$ {}^{CF}\mathbf{D}_t^b[g(ß)] = \frac{\mathcal{N}(b)}{1-b}\int_0^t g'(ß)\exp\left[-b\frac{t-\rho}{1-b}\right]dß,$$

where $\mathcal{N}(0) = \mathcal{N}(1) = 1$ is known as normalization function. Also for $g \in H^1[0,T]$, the the CF can be described by

$$ {}^{CF}\mathbf{D}_t^b[g(ß)] = \frac{\mathcal{N}(b)}{1-b}\int_0^t \Big(g(ß)-g(\rho)\Big)\exp\left[-b\frac{t-\rho}{1-b}\right]d\rho,$$

Definition 2 *Let g be a function, then the fractional integral of CF with order $b \in (0,1)$ is given as*

$$ {}^{CF}\mathbf{I}_t^b[g(ß)] = \frac{1-b}{\mathcal{N}(b)} + \frac{b}{\mathcal{N}(b)}\int_0^t g(ß)dß, \quad t \geq 0.$$

Definition 3 *[43] The Laplace transform for the CF derivative can be defined as*

$$ [{}^{CF}\mathbf{D}_t^b g(ß)] = \frac{\sigma[g(ß)] - g(0)}{\sigma + b(1-\sigma)}, \quad \sigma \geq 0.$$

3 Theoretical results

In this part, we will convert the considered model (1) into fractional form. By using the fractional operator in the framework of *CF* by including order b such that $0 < b \leq 1$ is given as:

$$\begin{cases} {}^{CF}\mathbf{D}_t^b\tilde{\mathbb{S}}(t) = \Pi + \alpha_1 - (\tau + \beta q)\tilde{\mathbb{S}}, \\ {}^{CF}\mathbf{D}_t^b\tilde{\mathbb{E}}(t) = \beta q\tilde{\mathbb{S}} - (\alpha_1 + \vartheta + (1-\kappa)\tau)\tilde{\mathbb{E}}, \\ {}^{CF}\mathbf{D}_t^b\tilde{\mathbb{I}}(t) = \tau\tilde{\mathbb{S}} + \tau(1-\kappa)\tilde{\mathbb{E}} - (\upsilon + \alpha_1 + \rho)\tilde{\mathbb{I}}, \\ {}^{CF}\mathbf{D}_t^b\tilde{\mathbb{R}}(t) = \vartheta\tilde{\mathbb{E}} - \alpha_1\tilde{\mathbb{R}} + \upsilon\tilde{\mathbb{I}}, \\ {}^{CF}\mathbf{D}_t^b\tilde{\mathbb{D}}(t) = \rho\tilde{\mathbb{I}} - \alpha_2\tilde{\mathbb{D}}, \\ {}^{CF}\mathbf{D}_t^b\tilde{\mathbb{M}}(t) = \sigma\tilde{\mathbb{E}} + \zeta\tilde{\mathbb{I}} - \varphi\tilde{\mathbb{M}}, \end{cases} \tag{2}$$

with initial conditions

$$\tilde{\mathbb{S}}_0 = \tilde{\mathbb{S}}(0), \quad \tilde{\mathbb{E}}_0 = \tilde{\mathbb{E}}(0), \quad \tilde{\mathbb{I}}_0 = \tilde{\mathbb{I}}(0), \quad \tilde{\mathbb{R}}_0 = \tilde{\mathbb{R}}(0), \quad \tilde{\mathbb{D}}_0 = \tilde{\mathbb{D}}(0), \quad \tilde{\mathbb{M}}_0 = \tilde{\mathbb{M}}(0).$$

In this part of the manuscript, we first determine whether the solution to the problem under investigation really exists or not. We exploit the approach of fixed point theory to determine the existence along with the uniqueness of the model. To develop the existence theory we will apply Picard's operator technique. In order to make mathematical analysis more efficient, we assume

that $\alpha_1 = \alpha_2 = \alpha$. To do this, we re-write the suggested model as

$$\begin{aligned}
{}^{CF}\mathbf{D}_t^b\tilde{\mathbb{S}}(t) &= \mathbf{V}_1(t,\tilde{\mathbb{S}}) = \Pi - (\tau + \alpha + \beta q)\tilde{\mathbb{S}},\\
{}^{CF}\mathbf{D}_t^b\tilde{\mathbb{E}}(t) &= \mathbf{V}_2(t,\tilde{\mathbb{E}}) = \beta q\tilde{\mathbb{S}} - (\vartheta + (1-\kappa)\tau + \alpha)\tilde{\mathbb{E}},\\
{}^{CF}\mathbf{D}_t^b\tilde{\mathbb{I}}(t) &= \mathbf{V}_3(t,\tilde{\mathbb{I}}) = \tau\tilde{\mathbb{S}} + \tau(1-\kappa)\tilde{\mathbb{E}} - (\alpha + \upsilon + \rho)\tilde{\mathbb{I}},\\
{}^{CF}\mathbf{D}_t^b\tilde{\mathbb{R}}(t) &= \mathbf{V}_4(t,\tilde{\mathbb{R}}) = \vartheta\tilde{\mathbb{E}} - \alpha\tilde{\mathbb{R}} + \upsilon\tilde{\mathbb{I}},\\
{}^{CF}\mathbf{D}_t^b\tilde{\mathbb{D}}(t) &= \mathbf{V}_5(t,\tilde{\mathbb{D}}) = \rho\tilde{\mathbb{I}} - \alpha\tilde{\mathbb{D}},\\
{}^{CF}\mathbf{D}_t^b\tilde{\mathbb{M}}(t) &= \mathbf{V}_6(t,\tilde{\mathbb{M}}) = \sigma\tilde{\mathbb{E}} + \zeta\tilde{\mathbb{I}} - \varphi\tilde{\mathbb{M}}.
\end{aligned} \tag{3}$$

In the following we set

$$F_i = \sup_{C[d,b_i]} \|\mathbf{V}_1(t,\tilde{\mathbb{S}})\|, \quad \text{for} \quad 1 \le j \le 6, \tag{4}$$

where

$$C[w,h_i] = [t-w, t+w] \times [u-c_i, u+c_i] = W \times W_i, \quad \text{for} \quad j = 1,2,\ldots,6. \tag{5}$$

Further, to demonstrate the existence as well as uniqueness of the concerned solution we define the norm on $C[w,h_i]$ where $1 \le j \le 6$ as follows

$$\|\mho\|_\infty = \sup_{t\in[t-w,t+h]} |\Phi(t)|. \tag{6}$$

The Picard operator is described by the expression

$$\mathbf{A} : C(W,W_1,W_2,W_3,W_4,W_5,W_6) \to C(W,W_1,W_2,W_3,W_4,W_5,W_6). \tag{7}$$

Applying ${}^{CF}\mathbf{I}^b$ to all Eqns. of the considered system (2) and using (3), we obtain

$$\begin{cases}
\tilde{\mathbb{S}}(t) = \tilde{\mathbb{S}}(0) + {}^{CF}\mathbf{I}^b[\mathbf{V}_1(t,\tilde{\mathbb{S}})],\\
\tilde{\mathbb{E}}(t) = \tilde{\mathbb{E}}(0) + {}^{CF}\mathbf{I}^b[\mathbf{V}_2(t,\tilde{\mathbb{E}})],\\
\tilde{\mathbb{I}}(t) = \tilde{\mathbb{I}}(0) + {}^{CF}\mathbf{I}^b[\mathbf{V}_3(t,\tilde{\mathbb{I}})],\\
\tilde{\mathbb{R}}(t) = \tilde{\mathbb{R}}(0) + {}^{CF}\mathbf{I}^b[\mathbf{V}_4(t,\tilde{\mathbb{R}})],\\
\tilde{\mathbb{D}}(t) = \tilde{\mathbb{D}}(0) + {}^{CF}\mathbf{I}^b[\mathbf{V}_5(t,\tilde{\mathbb{D}})],\\
\tilde{\mathbb{M}}(t) = \tilde{\mathbb{M}}(0) + {}^{CF}\mathbf{I}^b[\mathbf{V}_6(t,\tilde{\mathbb{M}})].
\end{cases} \tag{8}$$

Simplifying the RHS of the above equation we have

$$\Omega(t) = \Omega_0(t) + [\Upsilon(t,\Omega(t)) - \Upsilon_0(t)]\frac{1-b}{\mathcal{N}(b)} + \frac{b}{\mathcal{N}(b)}\int_0^t \Upsilon(x,\Omega(x))dx, \tag{9}$$

where

$$\begin{cases}
\Omega(t) = (\tilde{\mathbb{S}},\tilde{\mathbb{E}},\tilde{\mathbb{I}},\tilde{\mathbb{R}},\tilde{\mathbb{D}},\tilde{\mathbb{M}},)^T,\\
\Omega_0(t) = (\tilde{\mathbb{S}}_0,\tilde{\mathbb{E}}_0,\tilde{\mathbb{I}}_0,\tilde{\mathbb{R}}_0,\tilde{\mathbb{D}}_0\tilde{\mathbb{M}}_0)^T,\\
\Upsilon(t,\Omega(t)) = (\mathbf{V}_i(t,\tilde{\mathbb{S}},\tilde{\mathbb{E}},\tilde{\mathbb{I}},\tilde{\mathbb{R}},\tilde{\mathbb{D}},\tilde{\mathbb{M}})^T, \quad 1 \le i \le 6.
\end{cases} \tag{10}$$

Using Eq. (9) and Eq. (10), the operator defined in (7) can be expressed in the form

$$\mathbf{A}\Omega(t) = \Omega_0(t) + [\Upsilon(t,\Omega(t)) - \Upsilon_0(t)]\frac{1-b}{\mathcal{N}(b)} + \frac{b}{\mathcal{N}(b)}\int_0^t \Upsilon(ß,\Omega(ß))dß. \tag{11}$$

In the next step, we will assume that the considered system satisfies the following

$$\|\Omega\| \le \max\{w_1,w_2,w_3,w_4,w_5,w_6\}. \tag{12}$$

In this scenario, one may write

$$\begin{aligned}
\|\mathbf{A}\Omega - \Omega_0(t)\| &= \sup_{t\in D}\left|\Upsilon(t,\Omega(t))\frac{1-b}{\mathcal{N}(b)} + \frac{b}{\mathcal{N}(b)}\int_0^t \Upsilon(ß,\Omega(ß))dß\right|,\\
&\leq \frac{1-b}{\mathcal{N}(b)}\sup_{t\in D}|\Upsilon(t,\Omega(t))| + \frac{b}{\mathcal{N}(b)}\sup_{t\in D}\int_0^t |\Upsilon(ß,\Omega(ß))|dß,\\
&\leq \frac{1+t_0}{\mathcal{N}(b)}\mathcal{K}, \quad \mathcal{K} = \max\{\mathcal{K}_j\} \quad \text{for} \quad i = 1,2,\ldots,6\\
&< \mathcal{K}w \leq \max\{w_1,w_2,w_3,w_4,w_5,w_6\} = \overline{w}, \quad t_0 = \sup\{|t| : t \in W\}.
\end{aligned} \tag{13}$$

In the above Eq. (13), let us define $w = \frac{1+t_0}{\mathcal{N}(b)}$, we obtain

$$w < \frac{\overline{w}}{\mathcal{K}}.$$

Next, the given equality can be evaluated as

$$\|\mathbf{A}\Omega_1 - \mathbf{A}\Omega_2\| = \sup_{t\in W}|\Omega_1 - \Omega_2|, \tag{14}$$

we make the use of (9) and write

$$\begin{aligned}
\|\mathbf{A}\Omega_1 - \mathbf{A}\Omega_2\| &= \sup_{t\in W}\left|\frac{1-b}{\mathcal{N}(b)}(\Upsilon(t,\Omega_1(t))) - \Upsilon(t,\Omega_2(t))\right.\\
&+ \left.\frac{b}{\mathcal{N}(b)}\int_0^t(\Upsilon(ß,\Omega_1(ß))) - \Upsilon(ß,\Omega_2(ß))dß\right|\\
&\leq \frac{1-b}{\mathcal{N}(b)}k\sup_{t\in W}|\Omega_1(t) - \Omega_2(t)| + \frac{bk}{\mathcal{N}(b)}\sup_{t\in W}\int_0^t|\Omega_1(ß) - \Omega_2(ß)|dß, \quad \text{where} \quad k < 1\\
&\leq \left[\frac{1+t_0}{\mathcal{N}(b)}\right]k\|\Omega_1 - \Omega_2\|\\
&\leq wk\|\Omega_1 - \Omega_2\|.
\end{aligned} \tag{15}$$

Since Υ is a contraction, it follows that $wk < 1$. This reflects that the operator $\mathbf{A}$ is a contraction as well. Consequently one may conclude the uniqueness of the solution of the system under study.

4 Analytical algorithm for the proposed model

In the following, we focus our attention on finding the general series solution of the model. With the help of Laplace transform, the given system may be transformed into the form

$$\begin{aligned}
[\tilde{\mathbb{S}}(t)] &= \frac{\tilde{\mathbb{S}}(0)}{\sigma} + \frac{\sigma + b(1-\sigma)}{\sigma}[\Pi + \alpha - (\tau + \beta q)\tilde{\mathbb{S}}],\\
[\tilde{\mathbb{E}}(t)] &= \frac{\tilde{\mathbb{E}}(0)}{\sigma} + \frac{\sigma + b(1-\sigma)}{\sigma}[\beta q\tilde{\mathbb{S}} - (\vartheta + (1-\kappa)\tau + \alpha)\tilde{\mathbb{E}}],\\
[\tilde{\mathbb{I}}(t)] &= \frac{\tilde{\mathbb{I}}(0)}{\sigma} + \frac{\sigma + b(1-\sigma)}{\sigma}[\tau\tilde{\mathbb{S}} + \tau(1-\kappa)\tilde{\mathbb{E}} - (\alpha + \upsilon + \rho)\tilde{\mathbb{I}}],\\
[\tilde{\mathbb{R}}(t)] &= \frac{\tilde{\mathbb{R}}(0)}{\sigma} + \frac{\sigma + b(1-\sigma)}{\sigma}[\vartheta\tilde{\mathbb{E}} - \alpha\tilde{\mathbb{R}} + \upsilon\tilde{\mathbb{I}}],\\
[\tilde{\mathbb{D}}(t)] &= \frac{\tilde{\mathbb{D}}(0)}{\sigma} + \frac{\sigma + b(1-\sigma)}{\sigma}[\rho\tilde{\mathbb{I}} - \alpha\tilde{\mathbb{D}}],\\
[\tilde{\mathbb{M}}(t)] &= \frac{\tilde{\mathbb{M}}(0)}{\sigma} + \frac{\sigma + b(1-\sigma)}{\sigma}[\sigma\tilde{\mathbb{E}} + \zeta\mathbb{I} - \varphi\tilde{\mathbb{M}}].
\end{aligned} \tag{16}$$

Using the following series solution as

$$\begin{aligned}
\tilde{\mathbb{S}}(t) &= \sum_{z=0}^{\infty}\tilde{\mathbb{S}}_z(t), \quad \tilde{\mathbb{E}}(t) = \sum_{z=0}^{\infty}\tilde{\mathbb{E}}_z(t), \quad \tilde{\mathbb{I}}(t) = \sum_{z=0}^{\infty}\tilde{\mathbb{I}}_z(t), \quad \tilde{\mathbb{R}}(t) = \sum_{z=0}^{\infty}\tilde{\mathbb{R}}_z(t),\\
\tilde{\mathbb{D}}(t) &= \sum_{z=0}^{\infty}\tilde{\mathbb{D}}_z(t), \quad \tilde{\mathbb{M}}(t) = \sum_{z=0}^{\infty}\tilde{\mathbb{M}}_z(t).
\end{aligned} \tag{17}$$

Using equations (17), the system (16) has the following form:

$$\begin{aligned}
\left[\sum_{z=0}^{\infty}\tilde{\mathbb{S}}_z(t)\right] &= \frac{\tilde{\mathbb{S}}(0)}{\sigma} + \frac{\sigma + b(1-\sigma)}{\sigma}\left[\Pi - (\tau + \beta q + \alpha)\sum_{z=0}^{\infty}\tilde{\mathbb{S}}_z\right],\\
\left[\sum_{z=0}^{\infty}\tilde{\mathbb{E}}_z(t)\right] &= \frac{\tilde{\mathbb{E}}(0)}{\sigma} + \frac{\sigma + b(1-\sigma)}{\sigma}\left[\beta q\sum_{z=0}^{\infty}\tilde{\mathbb{S}}_z - (\vartheta + \alpha + (1-\kappa)\tau)\sum_{z=0}^{\infty}\tilde{\mathbb{E}}_z\right],\\
\left[\sum_{z=0}^{\infty}\tilde{\mathbb{I}}_z(t)\right] &= \frac{\tilde{\mathbb{I}}(0)}{\sigma} + \frac{s + b(1-\sigma)}{\sigma}\left[\tau\sum_{z=0}^{\infty}\tilde{\mathbb{S}}_z + (1-\kappa)\tau\sum_{z=0}^{\infty}\tilde{\mathbb{E}}_z - (\alpha + \rho + \upsilon)\sum_{z=0}^{\infty}\tilde{\mathbb{I}}_z\right],\\
\left[\sum_{z=0}^{\infty}\tilde{\mathbb{R}}_z(t)\right] &= \frac{\tilde{\mathbb{R}}(0)}{\sigma} + \frac{\sigma + b(1-\sigma)}{\sigma}\left[\vartheta\sum_{z=0}^{\infty}\tilde{\mathbb{E}}_z + \upsilon\sum_{z=0}^{\infty}\tilde{\mathbb{I}}_z - \alpha\sum_{z=0}^{\infty}\tilde{\mathbb{R}}_z\right],\\
\left[\sum_{z=0}^{\infty}\tilde{\mathbb{D}}_z(t)\right] &= \frac{\tilde{\mathbb{D}}(0)}{\sigma} + \frac{\sigma + b(1-\sigma)}{\sigma}\left[\rho\sum_{z=0}^{\infty}\tilde{\mathbb{I}}_z - \alpha\sum_{z=0}^{\infty}\tilde{\mathbb{D}}_z\right],\\
\left[\sum_{z=0}^{\infty}\tilde{\mathbb{M}}_z(t)\right] &= \frac{\tilde{\mathbb{M}}(0)}{\sigma} + \frac{\sigma + b(1-\sigma)}{\sigma}\left[\sigma\sum_{z=0}^{\infty}\tilde{\mathbb{E}}_z + \zeta\sum_{z=0}^{\infty}\tilde{\mathbb{I}}_z - \varphi\sum_{z=0}^{\infty}\tilde{\mathbb{M}}_z\right].
\end{aligned} \tag{18}$$

Comparing similar terms on both sides of (18), we may arrive at

$$\begin{aligned}
[\tilde{\mathbb{S}}_0(t)] &= \frac{\tilde{\mathbb{S}}_0}{\sigma}, \quad [\tilde{\mathbb{E}}_0(t)] = \frac{\tilde{\mathbb{E}}_0}{\sigma}, \quad [\tilde{\mathbb{I}}_0(t)] = \frac{\tilde{\mathbb{I}}_0}{\sigma}, \quad [\tilde{\mathbb{R}}_0(t)] = \frac{\tilde{\mathbb{R}}_0}{\sigma},\\
[\tilde{\mathbb{D}}_0(t)] &= \frac{\tilde{\mathbb{D}}_0}{\sigma}, \quad [\tilde{\mathbb{M}}_0(t)] = \frac{\tilde{\mathbb{M}}_0}{\sigma},\\
[\tilde{\mathbb{S}}_1(t)] &= \frac{\sigma + b(1-\sigma)}{\sigma}\left[\Pi - (\tau + \beta q + \alpha)\tilde{\mathbb{S}}_0\right],\\
[\tilde{\mathbb{E}}_1(t)] &= \frac{\sigma + b(1-\sigma)}{\sigma}\left[\beta q\tilde{\mathbb{S}}_0 - (\vartheta + \alpha + (1-\kappa)\tau)\tilde{\mathbb{E}}_0\right],\\
[\tilde{\mathbb{I}}_1(t)] &= \frac{\sigma + b(1-\sigma)}{\sigma}\left[\tau\tilde{\mathbb{S}}_0 + (1-\kappa)\tau\tilde{\mathbb{E}}_0 - (\alpha + \rho + \upsilon)\tilde{\mathbb{I}}_0\right],\\
[\tilde{\mathbb{R}}_1(t)] &= \frac{\sigma + b(1-\sigma)}{\sigma}\left[\vartheta\tilde{\mathbb{E}}_0 + \upsilon\tilde{\mathbb{I}}_0 - \alpha\tilde{\mathbb{R}}_0\right],\\
[\tilde{\mathbb{D}}_1(t)] &= \frac{\sigma + b(1-\sigma)}{\sigma}\left[\rho\tilde{\mathbb{I}}_0 - \alpha\tilde{\mathbb{D}}_0\right],\\
[\tilde{\mathbb{M}}_1(t)] &= \frac{\sigma + b(1-\sigma)}{\sigma}\left[\sigma\tilde{\mathbb{E}}_0 + \zeta\tilde{\mathbb{I}}_0 - \varphi\tilde{\mathbb{M}}_0\right],\\
[\tilde{\mathbb{S}}_2(t)] &= \frac{\sigma + b(1-\sigma)}{\sigma}\left[\Pi - (\tau + \beta q + \alpha)\tilde{\mathbb{S}}_1\right],\\
[\tilde{\mathbb{E}}_2(t)] &= \frac{\sigma + b(1-\sigma)}{\sigma}\left[\beta q\tilde{\mathbb{S}}_1 - (\vartheta + \alpha + (1-\kappa)\tau)\tilde{\mathbb{E}}_1\right],\\
[\tilde{\mathbb{I}}_2(t)] &= \frac{\sigma + b(1-\sigma)}{\sigma}\left[\tau\tilde{\mathbb{S}}_1 + (1-\kappa)\tau\tilde{\mathbb{E}}_1 - (\alpha + \rho + \upsilon)\tilde{\mathbb{I}}_1\right],\\
[\tilde{\mathbb{R}}_2(t)] &= \frac{\sigma + b(1-\sigma)}{\sigma}\left[\vartheta\tilde{\mathbb{E}}_1 + \upsilon\tilde{\mathbb{I}}_1 - \alpha\tilde{\mathbb{R}}_1\right],\\
[\tilde{\mathbb{D}}_2(t)] &= \frac{\sigma + b(1-\sigma)}{\sigma}\left[\rho\tilde{\mathbb{I}}_1 - \alpha\tilde{\mathbb{D}}_1\right],\\
[\tilde{\mathbb{M}}_2(t)] &= \frac{\sigma + b(1-\sigma)}{\sigma}\left[\sigma\tilde{\mathbb{E}}_1 + \zeta\tilde{\mathbb{I}}_1 - \varphi\tilde{\mathbb{M}}_1\right],\\
&\vdots\\
[\tilde{\mathbb{S}}_{q+1}(t)] &= \frac{\sigma + b(1-\sigma)}{\sigma}\left[\Pi - (\tau + \beta q + \alpha)\tilde{\mathbb{S}}_z\right],\\
[\tilde{\mathbb{E}}_{q+1}(t)] &= \frac{\sigma + b(1-\sigma)}{\sigma}\left[\beta q\tilde{\mathbb{S}}_z - (\vartheta + \alpha + (1-\kappa)\tau)\tilde{\mathbb{E}}_z\right],\\
[\tilde{\mathbb{I}}_{q+1}(t)] &= \frac{\sigma + b(1-\sigma)}{\sigma}\left[\tau\tilde{\mathbb{S}}_z + (1-\kappa)\tau\tilde{\mathbb{E}}_z - (\alpha + \rho + \upsilon)\tilde{\mathbb{I}}_z\right],\\
[\tilde{\mathbb{R}}_{q+1}(t)] &= \frac{\sigma + b(1-\sigma)}{\sigma}\left[\vartheta\tilde{\mathbb{E}}_z + \upsilon\tilde{\mathbb{I}}_z - \alpha\tilde{\mathbb{R}}_z\right],\\
[\tilde{\mathbb{D}}_{q+1}(t)] &= \frac{\sigma + b(1-\sigma)}{\sigma}\left[\rho\tilde{\mathbb{I}}_z - \alpha\tilde{\mathbb{D}}_z\right],\\
[\tilde{\mathbb{M}}_{q+1}(t)] &= \frac{\sigma + b(1-\sigma)}{\sigma}\left[\sigma\tilde{\mathbb{E}}_z + \zeta\tilde{\mathbb{I}}_z - \varphi\tilde{\mathbb{M}}_z\right].
\end{aligned} \tag{19}$$

On computing the Laplace transform of Eq. (19), we have

$$
\begin{aligned}
&\tilde{\mathbb{S}}_0(t) = \mathbb{N}_1,\ \tilde{\mathbb{E}}_0(t) = \mathbb{N}_2,\ \tilde{\mathbb{I}}_0(t) = \mathbb{N}_3,\ \tilde{\mathbb{R}}_0(t) = \mathbb{N}_4,\ \tilde{\mathbb{D}}_0(t) = \mathbb{N}_5,\ \tilde{\mathbb{M}}_0(t) = \mathbb{N}_6,\\
&\tilde{\mathbb{S}}_1(t) = \Big[\Pi - (\tau + \beta q + \alpha)\mathbb{N}_1\Big](1 + b(t-1)),\\
&\tilde{\mathbb{E}}_1(t) = \Big[\beta q\mathbb{N}_1 - (\alpha + \vartheta + (1-\kappa)\tau)\mathbb{N}_2\Big](1 + b(t-1)),\\
&\tilde{\mathbb{I}}_1(t) = \Big[\tau\mathbb{N}_1 + \tau(1-\kappa)\mathbb{N}_2 - (\rho + \alpha + \upsilon)\mathbb{N}_3\Big](1 + b(t-1)),\\
&\tilde{\mathbb{R}}_1(t) = \Big[\vartheta\mathbb{N}_2 + \upsilon\mathbb{N}_3 - \alpha\mathbb{N}_4\Big](1 + b(t-1)),\\
&\tilde{\mathbb{D}}_1(t) = \Big[\rho\mathbb{N}_3 - \alpha\mathbb{N}_5\Big](1 + b(t-1)),\\
&\tilde{\mathbb{M}}_1(t) = \Big[\sigma\mathbb{N}_2 + \zeta\mathbb{N}_3 - \varphi\mathbb{N}_6\Big](1 + b(t-1)),\\
&\tilde{\mathbb{S}}_2(t) = \Pi(1 + b(t-1))\Big[-(\tau + \beta q + \alpha)s_{11}\Big]\left(\frac{1}{2}b^2t^2 - 2b^2t + 2bt + (b-1)^2\right),\\
&\tilde{\mathbb{E}}_2(t) = \Big[\beta q s_{11} - (\vartheta + \alpha + (1-\kappa)\tau)e_{11}\Big]\left(\frac{1}{2}b^2t^2 - 2b^2t + 2bt + (b-1)^2\right),\\
&\tilde{\mathbb{I}}_2(t) = \Big[\tau s_{11} + \tau(1-\kappa)e_{11} - (\rho + \alpha + \upsilon)u_{11}\Big]\left(\frac{1}{2}b^2t^2 - 2b^2t + 2bt + (b-1)^2\right),\\
&\tilde{\mathbb{R}}_2(t) = \Big[\vartheta e_{11} + \upsilon u_{11} - \alpha r_{11}\Big]\left(\frac{1}{2}b^2t^2 - 2b^2t + 2bt + (b-1)^2\right),\\
&\tilde{\mathbb{D}}_2(t) = \Big[\rho u_{11} - \alpha d_{11}\Big]\left(\frac{1}{2}b^2t^2 - 2b^2t + 2bt + (b-1)^2\right),\\
&\tilde{\mathbb{M}}_2(t) = \Big[\sigma e_{11} + \zeta u_{11} - \varphi m_{11}\Big]\left(\frac{1}{2}b^2t^2 - 2b^2t + 2bt + (b-1)^2\right).
\end{aligned}
\tag{20}
$$

Correspondingly, the series solution for the next terms may be computed. Further, the unknown terms in the above equation (20) are as

$$
\begin{aligned}
s_{11} &= \Pi - (\tau + \beta q + \alpha)\mathbb{N}_1,\\
e_{11} &= \beta q\mathbb{N}_1 - (\alpha + \vartheta + \tau(1-\kappa))\mathbb{N}_2,\\
u_{11} &= \tau\mathbb{N}_1 + \tau(1-\kappa)\mathbb{N}_2 - (\rho + \alpha + \upsilon)\mathbb{N}_3,\\
r_{11} &= \vartheta\mathbb{N}_2 + \upsilon\mathbb{N}_3 - \alpha\mathbb{N}_4,\\
d_{11} &= \rho\mathbb{N}_3 - \alpha\mathbb{N}_5,\\
m_{11} &= \sigma\mathbb{N}_2 + \zeta\mathbb{N}_3 - \varphi\mathbb{N}_6.
\end{aligned}
\tag{21}
$$

5 Results and discussion

This particular section of the manuscript is devoted to the numerical simulations of the proposed model. Parameters of the model are assigned values given in Table 2 which are taken from [17]. The description of initial population of the compartments for the proposed model is $\tilde{\mathbb{S}} = 220.89857$, $\tilde{\mathbb{E}} = 220.812$, $\tilde{\mathbb{I}} = 0.0008555$, $\tilde{\mathbb{R}} = 0.00003208$, $\tilde{\mathbb{D}} = 0.0007777$, $\tilde{\mathbb{M}} = 80.000706$ million.

Parameters	values	Parameters	values
Π	0.80	β	0.000761
α	0.0080	τ	0.00073
ρ	0.00039	q	1
ϑ	0.00064	σ	0.0075
κ	0.5998	ζ	0.0023
φ	0.07862	υ	0.000236

Table 2. Parameter values used in numerical simulation

We simulate the six classes of the model under consideration for available data described in Table 2 using the series solution technique of Laplace transform. Figure 1 is the representation of the susceptible class showing sudden decay with the passing of time. This is due to the fact that various contaminated constituents of COVID-19 are absorbed by the said class and jump to the other classes of the system. At the early stage, they decrease and afterward the class becomes stable for distinct fractional-order b. Fractional order behavior is compared with integer order. In Figure 2 one can see the representation of exposed cases for different fractional-order b along with a comparison with integer-order. Like susceptible the exposed population also decreases as they transfer to other compartments. Figure 3 shows that the infection class reaches the maximum value. This class then slowly and gradually decreases and attains stability at various fractional orders. Due to the robust immunity and self-defense, there are

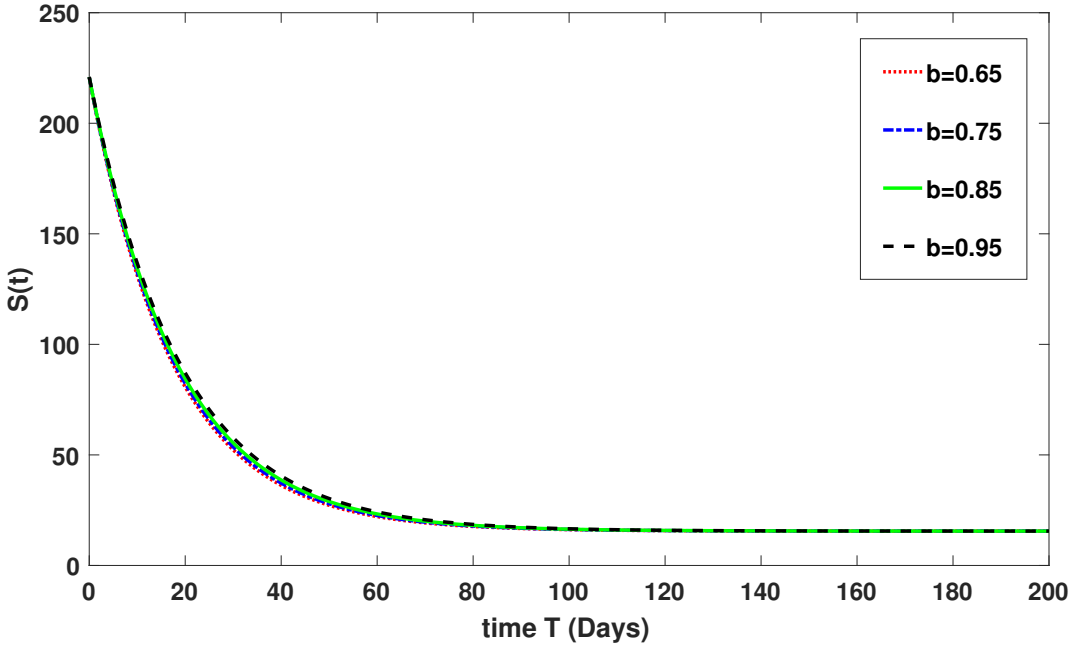

Figure 1. Dynamical behavior of $\tilde{\mathbb{S}}$ at various order b.

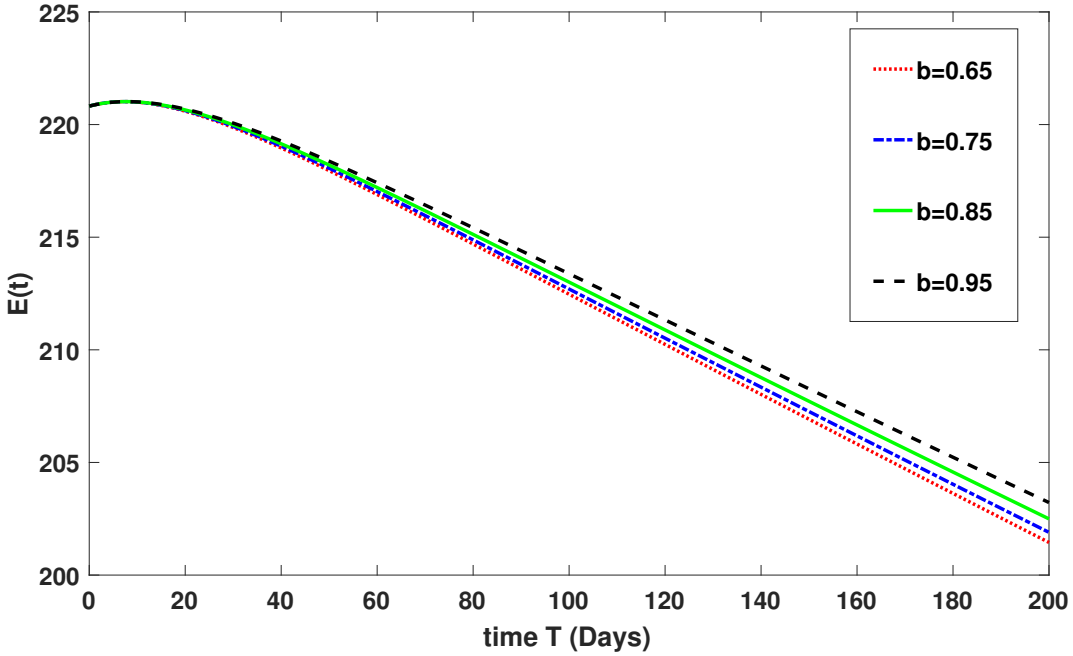

Figure 2. Dynamical behavior of $\tilde{\mathbb{E}}$ at various order b.

reductions and stability in the infection. Once more, we have provided an integer-order comparison. The recovery rate increases over time as the infection class increases. The maximum attained value for the recovered class is 1.5. After that, the recovery class also becomes stable as shown in Figure 4. We have observed in all the graphical representations that by increasing the values of fractional order, the dynamics will converge to the integer-order value 1. The stability was attained rapidly at low fractional-order and vice versa. Figure 5 represents the dynamics of demised class caused due to COVID-19. We note that the maximum value of this compartment is attained at 0.01. The class then declines and approaches the stability in distinct fractional orders. The decline

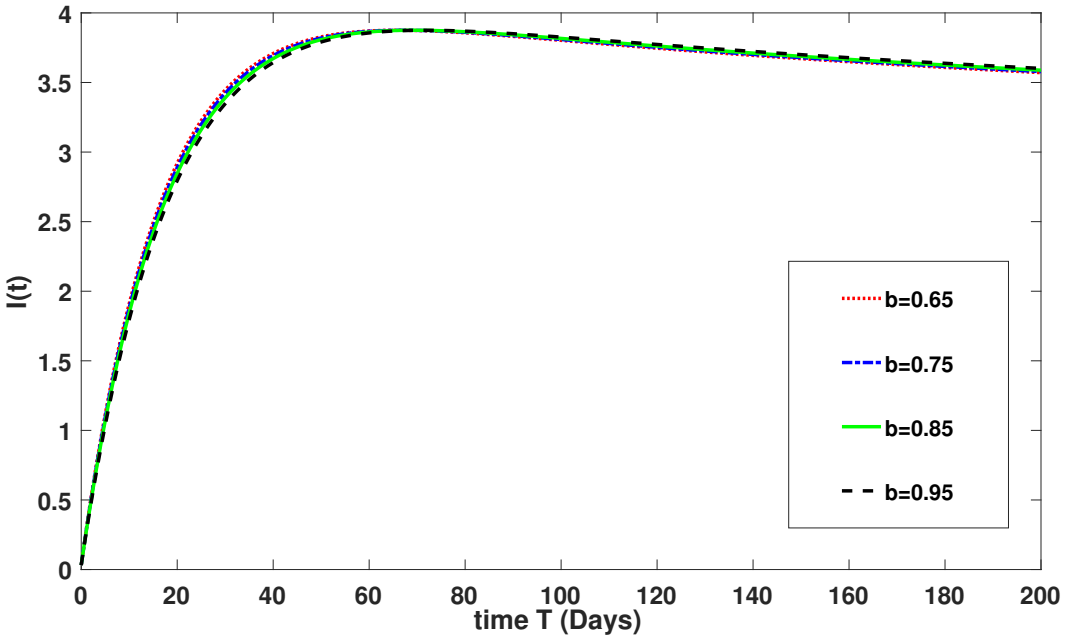

Figure 3. Dynamical behavior of $\tilde{\mathbb{I}}$ at various order b.

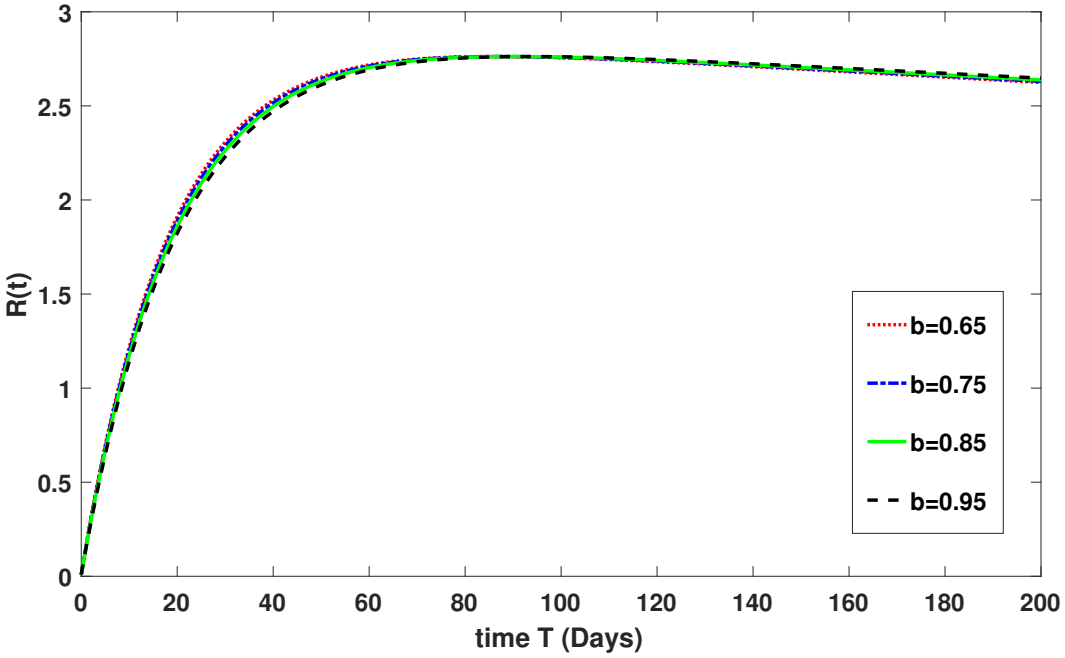

Figure 4. Dynamical behavior of $\tilde{\mathbb{I}}$ at various order b.

and stability gained in the demised class are due to the decrease in infection and the adoption of some precautionary measures for cleaning society. This obviously decreases the contaminated constituents $\tilde{\mathbb{M}}(t)$ as depicted in Figure 6. In Figures 7–12, we take another set of initial data as $\tilde{\mathbb{S}} = 220$, $\tilde{\mathbb{E}} = 150.892$, $\tilde{\mathbb{I}} = 0.4555$, $\tilde{\mathbb{R}} = 0.013208$, $\tilde{\mathbb{D}} = 0.7777$, $\tilde{\mathbb{M}} = 80.000706$ million. The behavior of all six compartments is slightly changed and converging on different fractional orders. In this case, we also compare the dynamics of fractional orders with integer orders.

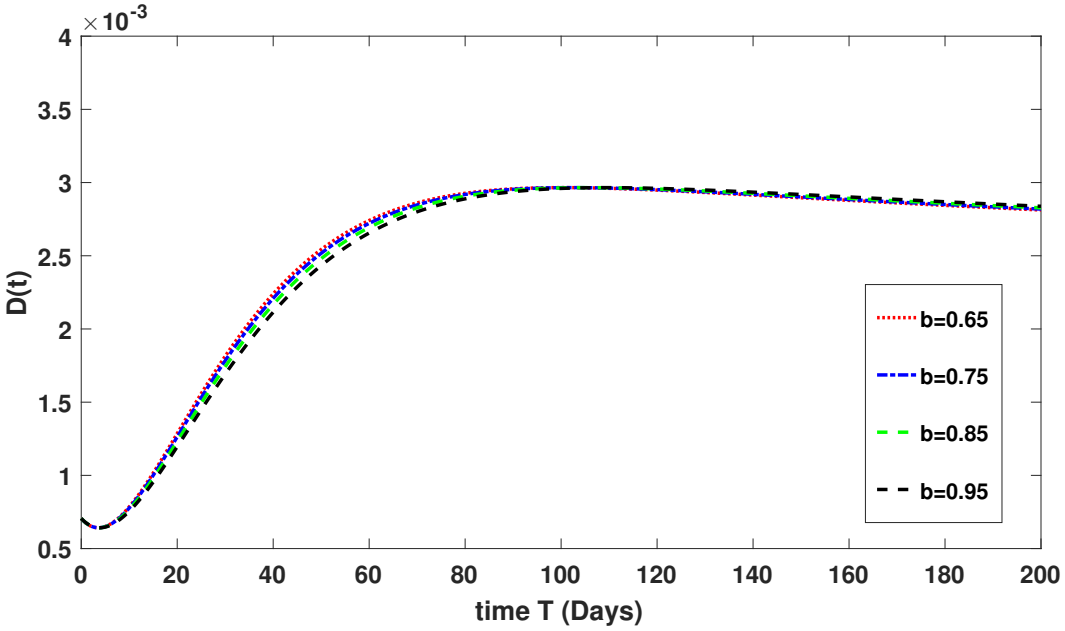

Figure 5. Dynamical behavior of $\tilde{\mathbb{D}}$ at various order b.

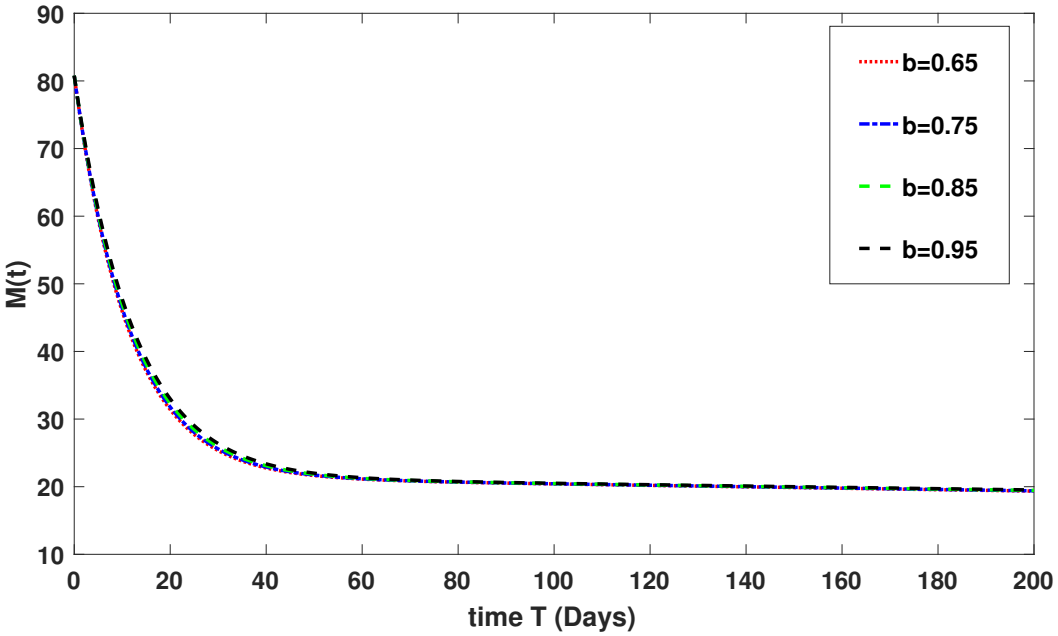

Figure 6. Dynamical behavior of $\tilde{\mathbb{M}}$ at various order b.

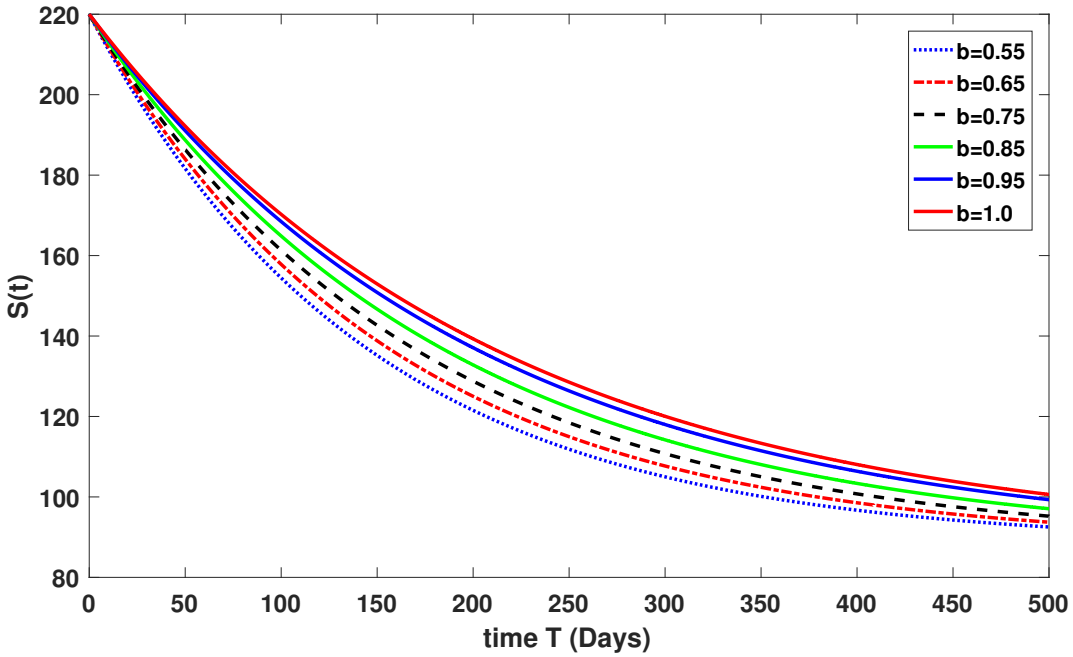

Figure 7. Dynamical behavior of $\tilde{\mathbb{S}}$ at various order b.

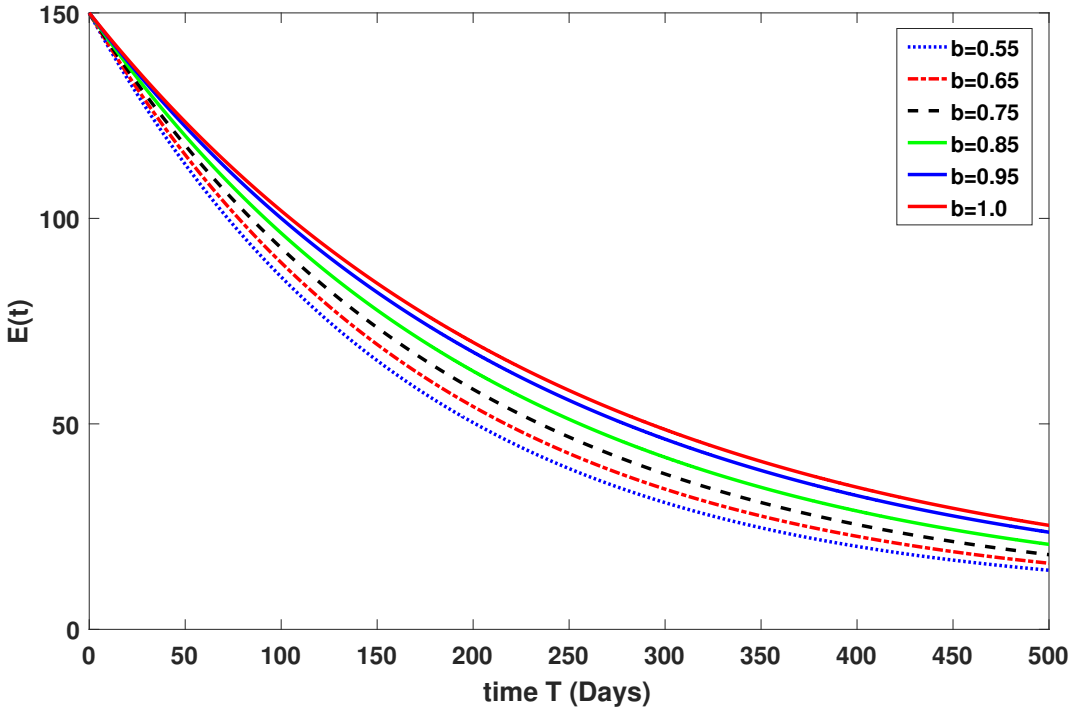

Figure 8. Dynamical behavior of $\tilde{\mathbb{E}}$ at various order b.

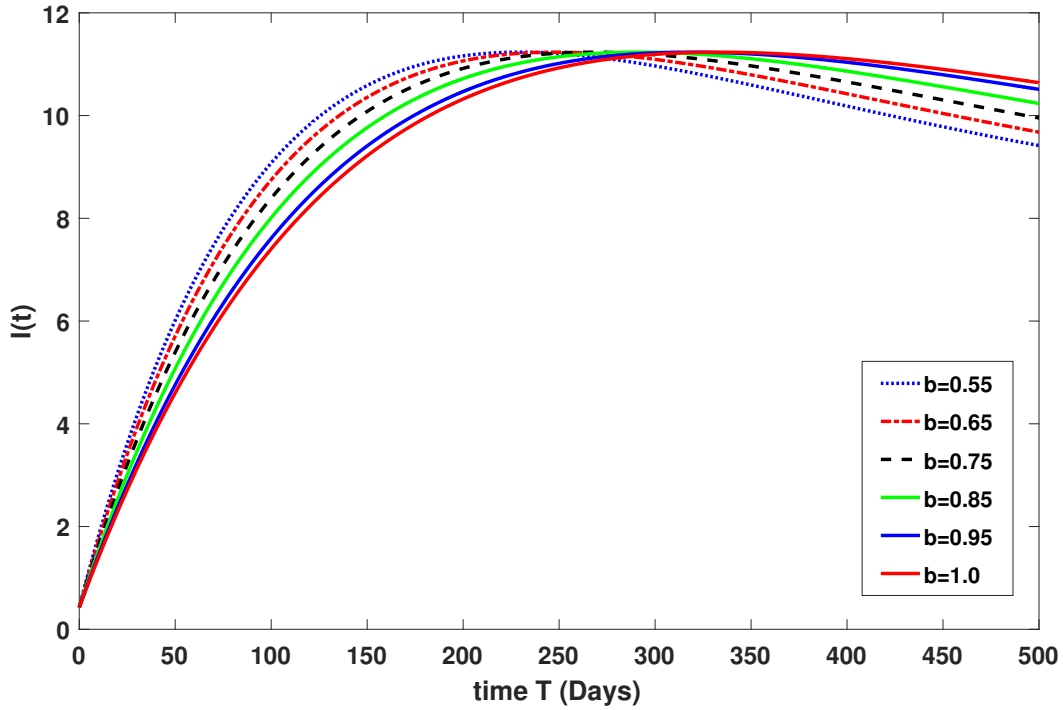

Figure 9. Dynamical behavior of $\tilde{\mathbb{I}}$ at various order b.

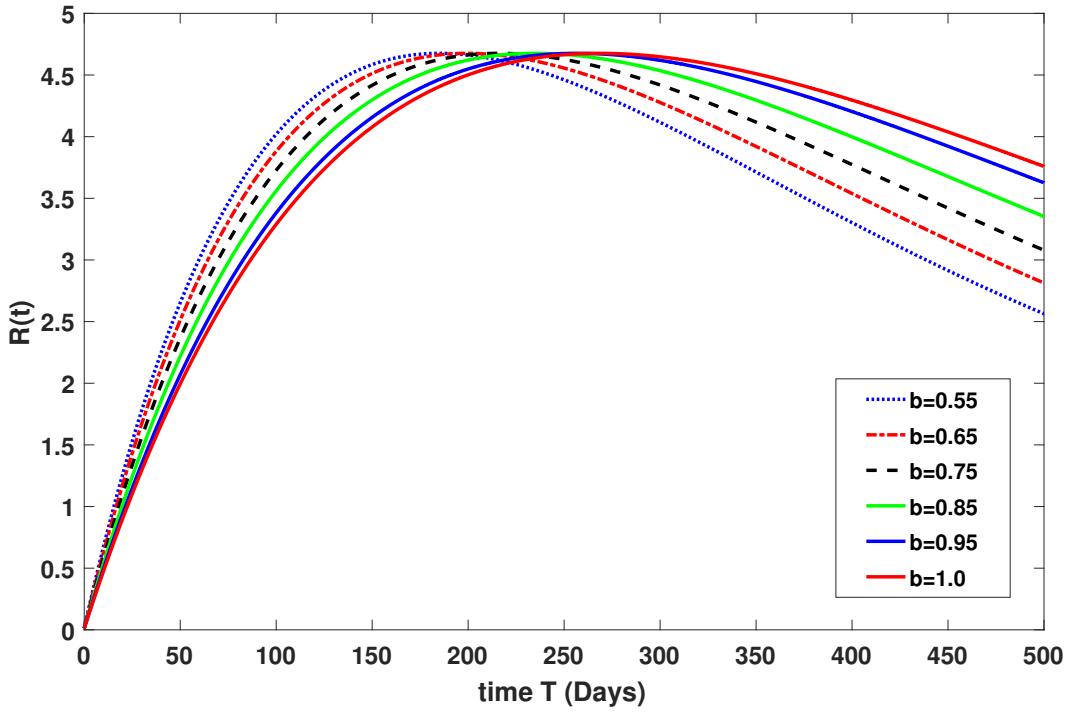

Figure 10. Dynamical behavior of $\tilde{\mathbb{R}}$ at various order b.

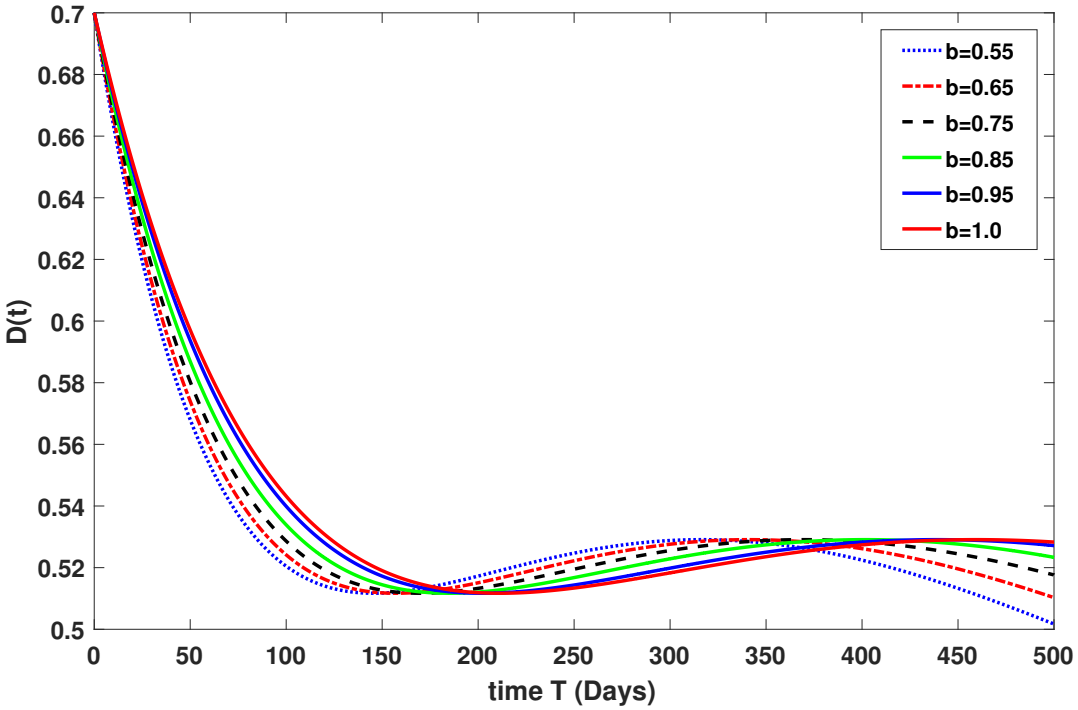

Figure 11. Dynamical behavior of $\tilde{\mathbb{D}}$ at various order b.

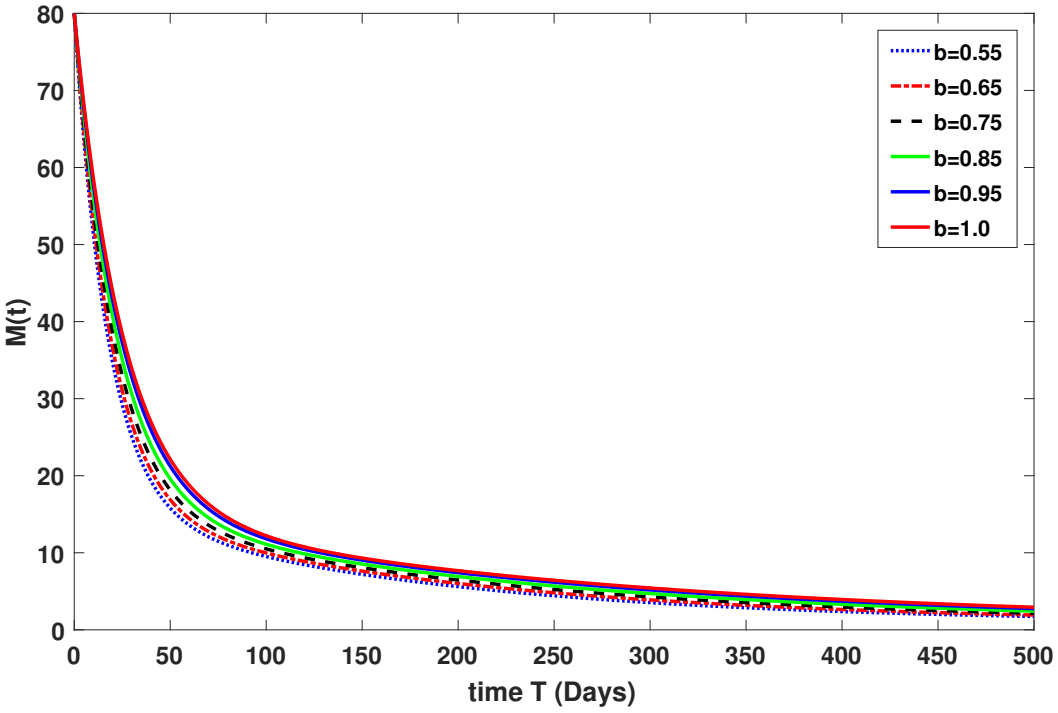

Figure 12. Dynamical behavior of $\tilde{\mathbb{M}}$ at various order b.

6 Conclusion

In this paper, we have examined the dynamics of a fractionally-order modified non-linear SEIR type system using the Caputo-Fabrizio derivative operator of the non-singular kernel. Our study suggested a strategy to overcome the spread of COVID-19 and how to stabilize it. We have carried out the qualitative analysis with the help of the findings from the nonlinear functional analysis. The numerical solutions have been obtained with the aid of the Laplace transform of series solutions. All the small quantities are then added together to obtain an approximate solution for each quantity. The said technique has been simulated for the first few terms on different fractional orders along with a comparison with integer orders to validate the required scheme. This dynamic is caused by viruses or microorganisms present in the human body and throat, therefore, the nano-technical dynamics of the pandemic model are very effective in the sense of fractional derivative. Therefore, our study has strongly recommended that an individual strictly follow the SOPs of the WHO in order to control the spread of the infection. It is also essential to raise awareness and disseminate information in society in order to keep the populace safe from the virus and possibly prevent the infection from spreading to a pandemic level. Our research predicts the future spread and controls of the COVID-19 dynamics in the form of a fractional Caputo-Fabrizio derivative for dynamics ranging from 0 to 1.

Declarations

Consent for publication

Not applicable.

Conflicts of interest

The authors declare that they have no conflict of interest.

Funding

Not applicable.

Author's contributions

S.A.: Writing-Original Draft, Methodology, Formal Analysis. D.Q.: Software, Formal Analysis, Conceptualization. M.U.R.: Writing-Review & Editing, Methodology, Formal Analysis. All authors discussed the results and contributed to the final manuscript.

Acknowledgements

This work was supported by the National Natural Science Foundation of China (Grant no. 12171065).

References

[1] World Health Organization, Coronavirus disease 2019 (COVID-19) Situation Report-62 *https : //www.who.int/docs/default – source/coronaviruse/situation – reports/20200322 – sitrep – 62 – covid – 19.pdf?sfvrsn = f7764c462*, 2020.

[2] Lu, H., Stratton, C.W., & Tang, Y.W. Outbreak of pneumonia of unknown etiology in Wuhan, China: The mystery and the miracle. *Journal of Medical Virology*, 92(4), 401-402, (2020). [CrossRef]

[3] Uçar, S. Analysis of hepatitis B disease with fractal–fractional Caputo derivative using real data from Turkey. *Journal of Computational and Applied Mathematics*, 419, 114692, (2023). [CrossRef]

[4] Uçar, E., Özdemir, N., & Altun, E. Qualitative analysis and numerical simulations of new model describing cancer. *Journal of Computational and Applied Mathematics*, 422, 114899, (2023). [CrossRef]

[5] Evirgen, F. Transmission of Nipah virus dynamics under Caputo fractional derivative. *Journal of Computational and Applied Mathematics*, 418, 114654, (2023). [CrossRef]

[6] Özköse, F., Yavuz, M., Şenel, M.T., & Habbireeh, R. Fractional order modelling of omicron SARS-CoV-2 variant containing heart attack effect using real data from the United Kingdom. *Chaos, Solitons & Fractals*, 157, 111954, (2022). [CrossRef]

[7] Joshi, H., Jha, B.K., & Yavuz, M. Modelling and analysis of fractional-order vaccination model for control of COVID-19 outbreak using real data. *Mathematical Biosciences and Engineering*, 20(1), 213-240, (2023). [CrossRef]

[8] Allegretti, S., Bulai, I.M., Marino, R., Menandro, M.A., & Parisi, K. Vaccination effect conjoint to fraction of avoided contacts for a Sars-Cov-2 mathematical model. *Mathematical Modelling and Numerical Simulation with Applications*, 1(2), 56-66, (2021). [CrossRef]

[9] Haq, I.U., Ali, N., & Nisar, K.S. An optimal control strategy and Grünwald-Letnikov finite-difference numerical scheme for the fractional-order COVID-19 model. *Mathematical Modelling and Numerical Simulation with Applications*, 2(2), 108-116, (2022). [CrossRef]

[10] He, F., Deng, Y., & Li, W. Coronavirus disease 2019: What we know?. *Journal of medical virology*, 92(7), 719-725, (2020). [CrossRef]

[11] Tian, X., Li, C., Huang, A., Xia, S., Lu, S., Shi, Z., ... & Ying, T. Potent binding of 2019 novel coronavirus spike protein by a SARS coronavirus-specific human monoclonal antibody. *Emerging microbes & infections*, 9(1), 382-385, (2020). [CrossRef]

[12] Riou, J., & Althaus, C.L. Pattern of early human-to-human transmission of Wuhan 2019 novel coronavirus (2019-nCoV), December 2019 to January 2020. *Eurosurveillance*, 25(4), 2000058, (2020). [CrossRef]

[13] Li, B., Liang, H., & He, Q. Multiple and generic bifurcation analysis of a discrete Hindmarsh-Rose model. *Chaos, Solitons & Fractals*, 146, 110856, (2021). [CrossRef]

[14] Eskandari, Z., Avazzadeh, Z., Khoshsiar Ghaziani, R., & Li, B. Dynamics and bifurcations of a discrete-time Lotka–Volterra model using nonstandard finite difference discretization method. *Mathematical Methods in the Applied Sciences*, (2022). [CrossRef]

[15] Li, B., Liang, H., Shi, L., & He, Q. Complex dynamics of Kopel model with nonsymmetric response between oligopolists. *Chaos, Solitons & Fractals*, 156, 111860, (2022). [CrossRef]

[16] Qu, H., Rahman, M.U., Wang, Y., Arfan, M., & Adnan. Modeling Fractional-Order Dynamics of Mers-Cov via Mittag-Leffler Law. *Fractals*, 30(1), 2240046, (2022). [CrossRef]

[17] Mekonen, K.G., Habtemicheal, T.G., & Balcha, S.F. Modeling the effect of contaminated objects for the transmission dynamics of COVID-19 pandemic with self protection behavior changes. *Results in Applied Mathematics*, 9, 100134, (2021). [CrossRef]

[18] Kilbas, A.A., Srivastava, H.M., & Trujillo, J.J. *Theory and applications of fractional differential equations* (Vol.204). Elsevier, (2006).

[19] Samko, S.G., Kilbas, A.A., & Marichev, O.I. *Fractional integrals and derivatives: theory and applications* (Vol.1). Switzerland: Gordon and Breach Science Publishers, Yverdon, (1993).

[20] Haq, I.U., Yavuz, M., Ali, N., & Akgül, A. A SARS-CoV-2 fractional-order mathematical model via the modified Euler method. *Mathematical and Computational Applications*, 27(5), 82, (2022). [CrossRef]

[21] Ucar, S., Evirgen, F., Özdemir, N., & Hammouch, Z. Mathematical analysis and simulation of a giving up smoking model within the scope of non-singular derivative. *Proceeding of the Institute of Mathematics and Mechanics*, 48, 84-99, (2022). [CrossRef]

[22] Uçar, E., Uçar, S., Evirgen, F., & Özdemir, N. A fractional SAIDR model in the frame of Atangana–Baleanu derivative. *Fractal and Fractional*, 5(2), 32, (2021). [CrossRef]

[23] Hilfer, R. (Ed.). *Applications of fractional calculus in physics*. *World scientific*, (2000).

[24] Uçar, S. Existence and uniqueness results for a smoking model with determination and education in the frame of non-singular derivatives. *Amer Inst Mathematical Sciences-AIMS*, 14(7), 2571-2589, (2021). [CrossRef]

[25] Sene, N. Theory and applications of new fractional-order chaotic system under Caputo operator. *An International Journal of Optimization and Control*, 12(1), 20-38, (2022). [CrossRef]

[26] Zhang, L., ur Rahman, M., Haidong, Q., & Arfan, M. Fractal-fractional Anthroponotic Cutaneous Leishmania model study in sense of Caputo derivative. *Alexandria Engineering Journal*, 61(6), 4423-4433, (2022). [CrossRef]

[27] Caputo, M., & Fabrizio, M. A new definition of fractional derivative without singular kernel. *Progress in Fractional Differentiation & Applications*, 1(2), 73-85, (2015). [CrossRef]

[28] Atangana, A., & Alkahtani, B.S.T. Analysis of the Keller–Segel model with a fractional derivative without singular kernel. *Entropy*, 17(6), 4439-4453, (2015). [CrossRef]

[29] Koca, I. Analysis of rubella disease model with non-local and non-singular fractional derivatives. *An International Journal of Optimization and Control: Theories & Applications (IJOCTA)*, 8(1), 17-25, (2018). [CrossRef]

[30] Baleanu, D., Mohammadi, H., & Rezapour, S. A mathematical theoretical study of a particular system of Caputo–Fabrizio fractional differential equations for the Rubella disease model. *Advances in Difference Equations*, 2020(1), 1-19, (2020). [CrossRef]

[31] Abro, K.A., & Atangana, A. A comparative analysis of electromechanical model of piezoelectric actuator through Caputo–Fabrizio and Atangana–Baleanu fractional derivatives. *Mathematical Methods in the Applied Sciences*, 43(17), 9681-9691, (2020). [CrossRef]

[32] Morales-Delgado, V.F., Gómez-Aguilar, J.F., Saad, K., & Escobar Jiménez, R.F. Application of the Caputo-Fabrizio and Atangana-Baleanu fractional derivatives to mathematical model of cancer chemotherapy effect. *Mathematical Methods in the Applied Sciences*, 42(4), 1167-1193, (2019). [CrossRef]

[33] Chasreechai, S., Sitthiwirattham, T., El-Shorbagy, M.A., Sohail, M., Ullah, U., & ur Rahman, M. Qualitative theory and approximate solution to a dynamical system under modified type Caputo-Fabrizio derivative. *AIMS Mathematics*, 7(8), 14376-14393, (2022). [CrossRef]

[34] Nisar, K.S., Ahmad, S., Ullah, A., Shah, K., Alrabaiah, H., & Arfan, M. Mathematical analysis of SIRD model of COVID-19 with Caputo fractional derivative based on real data. *Results in Physics*, 21, 103772, (2021). [CrossRef]

[35] Ameen, I.G., Sweilam, N.H., & Ali, H.M. A fractional-order model of human liver: Analytic-approximate and numerical solutions comparing with clinical data. *Alexandria Engineering Journal*, 60(5), 4797-4808, (2021). [CrossRef]

[36] Xu, C., Ur Rahman, M., Fatima, B., & Karaca, Y. Theoretical and numerical investigation of complexities in fractional-order chaotic system having torus attractors, *Fractals*, 30(07), 2250164, (2022). [CrossRef]

[37] Shah, K., Ali, A., Zeb, S., Khan, A., Alqudah, M.A., & Abdeljawad, T. Study of fractional order dynamics of nonlinear mathematical model. *Alexandria Engineering Journal*, 61(12), 11211-11224, (2022). [CrossRef]

[38] Shah, K., Jarad, F., & Abdeljawad, T. On a nonlinear fractional order model of dengue fever disease under Caputo-Fabrizio derivative. *Alexandria Engineering Journal*, 59(4), 2305-2313, (2020). [CrossRef]

[39] Liu, X., ur Rahman, M., Ahmad, S., Baleanu, D., & Nadeem Anjam, Y. A new fractional infectious disease model under the non-singular Mittag–Leffler derivative. *Waves in Random and Complex Media*, 1-27, (2022). [CrossRef]

[40] Rahman, M.U., Arfan, M., Deebani, W., Kumam, P., & Shah, Z. Analysis of time-fractional Kawahara equation under Mittag-Leffler Power Law. *Fractals*, 30(1), 2240021, (2022). [CrossRef]

[41] Rahman, M.U., Althobaiti, A., Riaz, M.B., & Al-Duais, F.S. A theoretical and numerical study on fractional order biological models with Caputo-Fabrizio derivative. *Fractal and Fractional*, 6(8), 446, (2022). [CrossRef]

[42] Rashid, S., Hammouch, Z., Aydi, H., Ahmad, A. G., & Alsharif, A.M. Novel computations of the time-fractional Fisher's model via generalized fractional integral operators by means of the Elzaki transform. *Fractal and Fractional*, 5(3), 94, (2021). [CrossRef]

[43] Losada, J., & Nieto, J.J. Properties of a new fractional derivative without singular kernel. *Progress in Fractional Differentiation & Applications*, 1(2), 87-92, (2015). [CrossRef]

Mathematical Modelling and Numerical Simulation with Applications (MMNSA) (https://www.mmnsa.org)